INFLUENCE OF PROFILE FEATURES ON LONGSHORE SEDIMENT TRANSPORT

João Mil-Homens[1], Roshanka Ranasinghe[1,2,3], J.S.M. van Thiel de Vries[1,4] and M.J.F. Stive[1]

Abstract

Longshore sediment transport (LST) is one of the main drivers of beach morphology. Bulk LST formulas are routinely used in coastal management/engineering studies to assess LST rates and gradients. However, there is still great uncertainty in LST estimation with these bulk formulas. This uncertainty may have two sources: 1) experimental errors in the measured values and 2) the effect of parameters that are not part of the formulas. In this study, we attempt to find the influence of profile related features in the LST rates that are not accounted for in the bulk formulas. These features may influence the type of wave breaking. A process-based model (UNIBEST-LT) is used to calculate LST rates on a large number of profiles measured on the Dutch coast, all forced with the same realistic wave climate. We found that the LST rates vary with the profiles. The value corresponding to the 95th percentile of the resulting distribution is 50% higher than one correspondent to the 5th percentile. The root mean square downward slope parameter showed the best correlation with LST rates.

Key words: longshore sediment transport, process based models, UNIBEST-LT, cross-shore profile features

1. Introduction

Longshore sediment transport (LST) dictates to a large extent whether shores erode, accrete or remain stable. In addition, large and/or persistent LST rates may have various other impacts, such as: inlet closure/migration, ebb/flood delta erosion/accretion, rotation of pocket beaches and headland sand bypassing. The calculation of LST rates is therefore a key component on most coastal engineering/planning studies.

There are two main approaches to estimate LST: bulk transport formulas which are basic models that assume a simplified representation of the physical processes and generally use empirical coefficients for calibration (e.g. the CERC (CERC, 1984), the Kamphuis (Kamphuis, 1991) and the Bayram (Bayram et al., 2007) formulas) and process-based models which intend to include a large number of physical processes such as shear stress, pickup, suspension, wave-current interaction, etc. (e.g. Deigaard et al. (1986), UNIBEST (WL|Delft Hydraulics, 1992) and GENESIS (Hanson, 1989)).

Both approaches are useful for coastal engineers. Bulk formulations are often used to make a first guess based on limited information and process-based models are generally expected to produce more accurate estimates and more information.

In the present, bulk formulas show great uncertainty. Using an extensive data set, Mil-Homens et al. (2013) concluded that about 42% of the predictions obtained by the CERC, Kamphuis and Bayram formulas differ by a factor greater than 2 with respect to measured values.

As input, bulk formulas usually require wave characteristics at the edge of the surf zone (e.g. breaking wave height, direction and period) and in some cases basic morphological variables (e.g. mean grain diameter, beach slope). The effects of more complex hydrodynamics associated with morphological features in the surf zone are not taken into account.

The objective of this study is to investigate whether there are any significant correlations between LST rates and cross-shore surf zone features such as beach slope, the presence and number of bars, and others.

[1]Faculty of Civil Engineering and Geosciences, Delft University of Technology, PO Box 5048, 2600 GA Delft, The Netherlands
[2]Department of Water Engineering, UNESCO-IHE, PO Box 3015, 2601 DA Delft, The Netherlands
[3]Harbour, Coastal and Offshore Engineering, Deltares, PO Box 177, 2600 MH Delft, The Netherlands
[4]Morphology and Sediment Dynamics, Deltares, PO Box 177, 2600 MH Delft, The Netherlands

We hypothesise that profile features may influence LST rates mainly by dictating the type of wave breaking. For this reason, we investigate profile features that may be related to the type of breaker, i.e., that are related with the bed slope at the breaking point. To accomplish this, we calculate LST rates in a large set of profiles surveyed in the Dutch coast using a process-based model (UNIBEST-LT). This model takes into account most of the physical processes known to influence LST. All calculations are performed under the same wave conditions, and using the same sediment characteristics.

2. Wave breaking and LST

Wave breaking generates turbulence that can propagate downwards in the water column and reach the bed, as observed by Melville et al. (2002).This turbulence can contribute for stirring the sediment from the bed. It has been shown in laboratory that the type of wave breaking influences the amount of suspended sediment: Ting (2001) concluded that plunging wave breakers generate considerably larger downward velocities when compared to spilling breakers and Smith et al. (2009) measured LST under spilling and plunging wave conditions and concluded that the latter was able to stir significantly larger amounts of sediment from the bed and generated larger LST rates.

The Iribarren number (eq.(1)), also known as surf similarity, is the most used indicator for the type of breaker. Battjes (1974) found that ξ_b is typically less than 0.4 for spilling breakers and typically ranges from 0.4 to 2.0 for plunging breakers. In eq.(1) m is beach slope, L_o is deep-water wavelength, and H_b is the breaker height.

$$\xi_b = \frac{m}{\sqrt{H_b / L_o}} \tag{1}$$

A possible relationship between LST rates and the Iribarren number has been discussed in several studies (e.g., Kamphuis et al., 1978; Vitale et al., 1981; Bodge, 1986). Kamphuis et al., (1978), Kamphuis et al., (1986) and others, attempted to incorporate the Iribarren number into the empirical coefficient in the CERC formula.

For irregular waves, the value often used for the slope is the average over the breaking zone, i.e., the breaking depth (d_b) divided by the distance from the still water line to the breaker (x_b). However, this average bed slope may be a misleading indicator for the dominant breaker type. Waves with different heights break at different locations and the slope at the breaker position can be very different from the average slope. If bars are present, it is likely that waves break over the seaward slope of the bar where the slope is steeper than the average.

The bed slope may influence LST through a different mechanism. In a steeper slope the surf zone is more concentrated, i.e., waves with different heights have breaking points that are closer to each other. Consequently, the energy dissipation occurs in a smaller area of the surf zone. The rate of energy dissipation (proportional to the cross-shore gradient of the shear stress component S_{xy} of the radiation stress) is responsible for driving wave generated alongshore currents (Longuet-Higgins, 1970). In a more concentrated surf zone, there will be a more localized and stronger current exactly in the area where more sediment is in suspension.

In this study we investigate two types of profile related parameters: directly measured slope parameters and parameters that affect in an indirect way the slope, e.g., number of bars and another bar related parameter.

3. Model

The process-based model UNIBEST-LT computes the tide and wave induced alongshore currents and resulting sediment transport for a given cross-shore beach profile assuming that the beach is uniform in alongshore direction. The longshore sediment transport and its cross-shore distribution can be calculated using various transport formulas.

3.1. Wave propagation and surf zone dynamics

UNIBEST-LT computes the surf zone dynamics through a built-in wave propagation and decay model (Stive et al., 1984). This model takes into account the main processes affecting wave propagation: refraction, shoaling and dissipation due to wave breaking and bottom friction. The wave induced time-averaged alongshore current distribution is derived from a simplified momentum equation that reduces to a balance between cross-shore gradient of the alongshore momentum flux and alongshore bottom stress.

3.2. LST rates calculation

LST rates are calculated according to several total-load sediment transport formulations for sand and shingle. All formulas use a threshold for initiation of motion and a limitation of the flow capacity to carry sediment. The sediment transport is assumed to respond to local wave and current conditions in an instantaneous quasi-steady way.

The formulation identified as Van Rijn 2004 (Rijn, 2007a; Rijn, 2007b; Rijn, 2007c) is used in this study. It accounts for most of the physical processes known to be involved in sediment transport. The main features of this model are:

- intra-wave approach to bed-load transport with initiation of motion and estimation of effective bed-roughness (accounts for the effect of bed forms such as ripples)
- suspended-load transport calculation using a vertical concentration distribution (including effects like sediment mixing due to currents and waves, flocculation, hindered settling and stratification)
- consideration of sediment grading in the bed

3.3. Modelling wave breaking and sediment suspension

It is important for this study to understand how the model simulates wave breaking and its contribution to sediment suspension.

The wave propagation model includes wave breaking through a dissipation term added to the wave energy balance equation (eq.(2)).

$$\frac{d}{dx}\left(\frac{E}{\omega_r}c_g\cos\alpha\right)+\frac{D_b}{\omega_r}+\frac{D_f}{\omega_r}=0 \tag{2}$$

In eq.2 E is the wave energy per unit area, ω_r is the relative wave peak frequency, α is the wave angle, c_g the group velocity, D_f and D_b represent energy dissipation due to bottom friction and wave breaking (eq.(3)), respectively. The adopted referential uses x and y for the cross-shore and alongshore directions respectively.

$$D_b=\frac{1}{4}\rho g a_c Q_b\left(\frac{\omega_r}{2\pi}\right)H_m^2 \tag{3}$$

In eq.3 ρ is the density of water, g is the acceleration of gravity, a_c is a coefficient for wave breaking, Q_b is local fraction of breaking waves and H_m is the depth limited wave height. The local fraction of breaking waves introduces a dependency on the local slope. As mentioned in section 1, the steeper the slope the more concentrated the surf zone, the higher the local fraction of breaking waves and consequently the higher the value of D_b. This has an important effect on the calculation of the alongshore current. The alongshore current is a sum of the contribution of wave and tide generated currents (Eq.(4)):

$$V(x)=\frac{dS_{xy}}{dx}+f\left(\frac{dh_0}{dy}\right) \tag{4}$$

where $S_{xy}=En\sin\alpha\cos\alpha$ and dh_0/dy is the tidal alongshore surface slope. S_{xy} is directly dependent on D_b (eq.2).

The suspension of sediment is simulated within the sediment transport formulation. The effect of wave breaking on the Van Rijn (2004) (Rijn, 2007a; Rijn, 2007b; Rijn, 2007c) formulation is accounted for through a sediment mixing coefficient (eq.(5)):

$$\varepsilon_{s,cw} = \sqrt{\varepsilon_{s,c}{}^2 + \varepsilon_{s,w}{}^2} \tag{5}$$

where $\varepsilon_{s,c}$ and $\varepsilon_{s,w}$ are the current and wave sediment mixing coefficients. The wave mixing coefficient is different for the bed (eq.(6)) and upper (eq.(7)) parts of the water column:

$$\varepsilon_{s,w,bed} = 0.018\gamma_{br}\beta_w\delta_S U_{\delta,r} \tag{6}$$

$$\varepsilon_{s,w,\max} = 0.035\gamma_{br} h H_s / T_p \quad \text{with} \quad \varepsilon_{s,w,\max} \le 0.05 \text{ m}^2/\text{s} \tag{7}$$

where γ_{br} is an empirical coefficient related to wave breaking, β_w is a coefficient dependent on the sediment fall velocity, δ_S is the thickness of the mixing layer (also dependent on γ_{br}), $U_{\delta,r}$ is the representative near-bed peak orbital velocity based on significant wave height, h is the water depth, H_s is the significant wave height and T_p the peak period. The empirical coefficient related to wave breaking γ_{br} may account for differences in breaker type, but this dependency is not explicit in the equations. In Section 2 we refer to some studies that indicate that such dependency is expected to occur.

4. Data

Bathymetry profiles and wave climate data are the inputs to the numerical model. The bathymetry profiles used in this study are part of the JARKUS data set. This data set comprises profiles surveyed every year since 1965, along the entire Dutch coast. The profiles are separated by 250 m in the alongshore direction and, in the cross-shore direction, the points have a grid spacing of 5 m in the beach area and surf zone. In earlier measurements it is common to find a cross-shore grid spacing of 10 m in the points below NAP[5]. The profiles start inland in the dune area, and extend to depths of up to 18 m NAP in the most recent surveys. In general, profiles measured earlier stop at smaller depths and have lower quality data (less data points, more fluctuations). For this reason, we only used profiles that reach at least 8 m of depth. We considered the 8 m depth also to be the limit of the active profile. This limit was chosen based on Hinton et al., (1998), that found the depth of closure in the Holland coast to be between 5 m and 8 m, for a time scale of 20 years.

For this study, we only used profiles that: 1) are located between IJmuiden and Hoek van Holland, 2) have its most offshore point deeper than 8 m, 3) have at least 30 points with elevation below NAP, 4) have at least 5 points with elevation above NAP and that are at least 4 km away from the breakwaters at Hoek van Holland or IJmuiden. The total number of profiles that satisfy these conditions is 2888.

The model used a wave climate composed of 9 months of wave observations, from September 1999 to May 2000, normalized to one year. The wave data was collected by Rijkswaterstaat near IJmuiden.

5. Method

The UNIBEST-LT model was used to calculate LST rates for all the 2888 JARKUS profiles considered. For each profile used, we tried to identify and parameterise the most important profile features.

5.1. Model setup

In all computations the same input coefficients and wave forcing were used. The only difference between computations was the profile used. Tables 1 and 2 show the model parameters adopted in the simulations. The sediment properties we used are typical values for the Dutch coast.

Because the aim of this work is to study the differences between results and not the absolute values of LST rates, the value of the input parameters is not crucially important. Nevertheless, we took care that

[5]Nieuw Amsterdams Peil – reference level in the Netherlands

sediment related parameters have realistic values.

Table 1. Values used for the Van Rijn (2004) formula

D_{10}	D_{50}	D_{90}	D_{ss}	ρ_{water}	$\rho_{sediment}$	porosity	temperature	Salinity
140 μm	225 μm	280 μm	200 μm	1025 kg/m^3	2650 kg/m^3	0.4	15° C	30 ppm

Table 2. Values used for the wave parameters in UNIBEST-LT

γ	α	f_w	k_b
0.8	1	0	0.1 m

In Tables 1 and 2: D_{10}, D_{50} and D_{90} are the 10th, 50th and 90th percentiles of the grain size distribution, D_{ss} is the median size of suspended sediment, ρ_{water} and $\rho_{sediment}$ are the densities of water and sediment, γ is a wave breaking coefficient, α is another wave breaking coefficient, f_w is a coefficient for bottom friction and k_b is the bottom roughness.

Input files for the model were created with Python scripts. In this step, the grid that the model uses, the transport truncation point and dynamic boundary were defined. The model uses a flexible grid that allows the use of smaller cells near the shoreline and larger cells in deeper positions. Table 3 shows the reference grid sizes used in our simulations.

Table 3. Reference grid sizes used in the computations (cross-shore position is positive in the onshore direction, and zero represents the shoreline)

Cell size (m)	40	2	4	5	50	100
Cross-shore position (m)	10	0	-300	-500	-1000	-1800

5.2. Bar detection

The detection of bars is not straightforward. There is some ambiguity in what is considered a bar. In order to have an objective measure, we used the following method: 1) the profile was interpolated in a 5m grid (to avoid problems of missing values), 2) using a moving average method, the profile was smoothed to eliminate fluctuations due to measurement errors, 3) all local maxima (crests) and minima (troughs) were listed, 4) a relative height parameter r_{ct} was calculated using eq.(8), where d_{crest} and d_{trough} are the depths at the crest and at the trough respectively and 5) a threshold value for the ratio r_{ct} was set. Local maxima that have a relative height greater than the threshold are considered bars. The threshold adopted (via trial and error) was 0.1, but other values were also tested. Figure 1 shows an example of the results of the method.

$$r_{ct} = \frac{d_{crest} - d_{trough}}{d_{crest}} \tag{8}$$

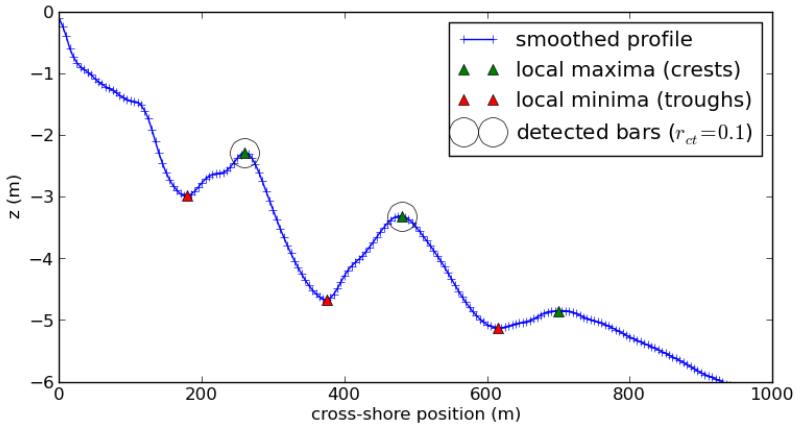

Figure 1. Example of the results obtained with the bar detection method. Notice that the last maximum was not considered a bar.

6. Results

6.1. LST rates

Figure 2 shows the distribution of LST rates obtained. LST rates range from 500 000 to more than 1000 000 m^3/y, and approximately 50% of LST rates are concentrated between 600 000 and 700 000 m^3/y. The 95th percentile is 895 000 m^3/y, approximately 50% higher than the 5th percentile, that is 595 000 m^3/y. Because the wave climate used as input is composed by a large variety of conditions, we think that these differences are mainly a consequence of differences in the profiles. However, it is possible that part of this variability is due to wave climate effects.

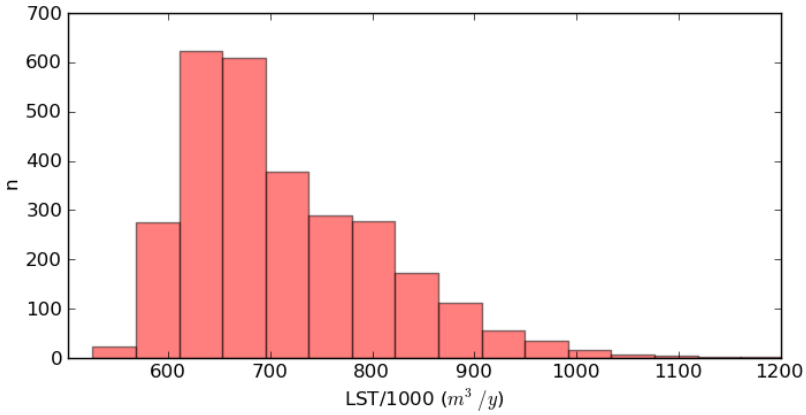

Figure 2. Distribution of the LST rates obtained.

6.2. Profile features

The profiles features chosen to be tested are: average slope, root mean square slope, average down slope, root mean square down slope, number of bars and the sum of the all r_{ct} (eq.(8)) values calculated for one profile.

The average slope was calculated with the formula: $m=x_{max}/h_{max}$ where x_{max} is the cross-shore position at a depth of h_{max}=8m. Figure 3 shows the scatter and the linear regression obtained between LST rates and average slope.

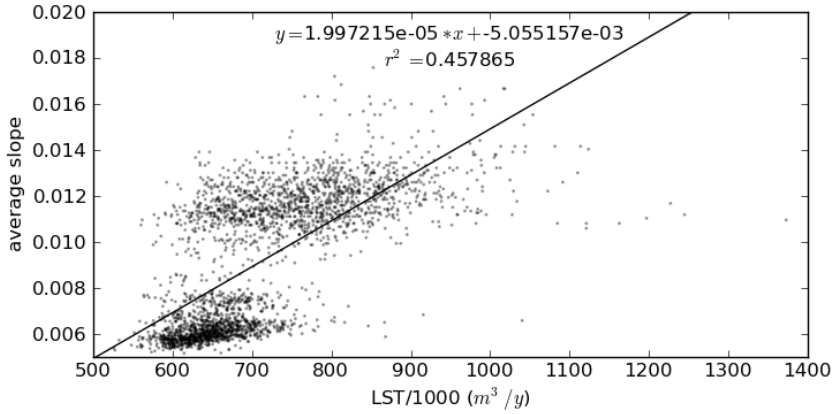

Figure 3. LST rates vs. average slope with linear regression

The *root mean square* slope is calculated on the smoothed profile, using the expression:

$$m_{rms} = \sqrt{\frac{\sum_n m_n^2}{n}} \tag{9}$$

where m_n are the slope values in each grid cell. Only cells over the active profile (until the 8 m depth) are considered. The *root mean square* accounts for variations of the slope value. Profiles with high slope variation have higher *root mean square* values. We used the smoothed profile because measurement errors can influence this measure. Figure 4 shows the scatter and linear regression results.

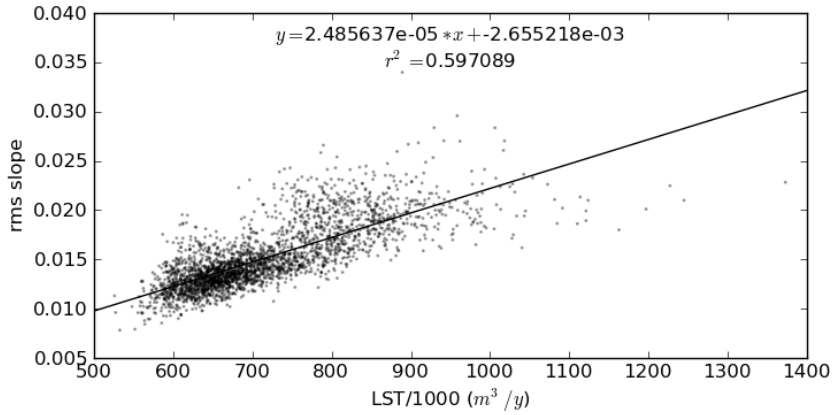

Figure 4. LST rates vs. *rms* slope with linear regression

Figure 5 presents the results for the average downwards slope, i.e., the average slope value of the grid cells that have a negative slope, over the active profile (until the 8 m depth). Grid cells with positive slopes are discarded (e.g. cells on the landward slope of a bar). Waves break where the slope is negative. It is expectable that the slope of those locations is a more accurate indicator for the type of breaker.

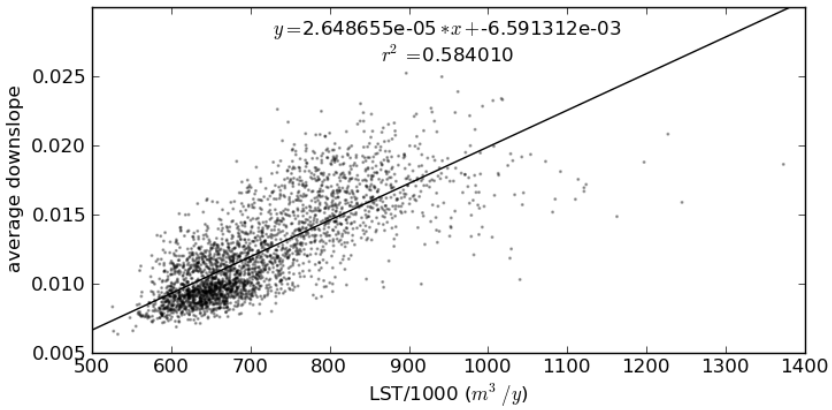

Figure 5. LST rates vs. average downwards slope with linear regression

Figure 6 shows the *root mean square* downwards slope scatter and the linear regression result.

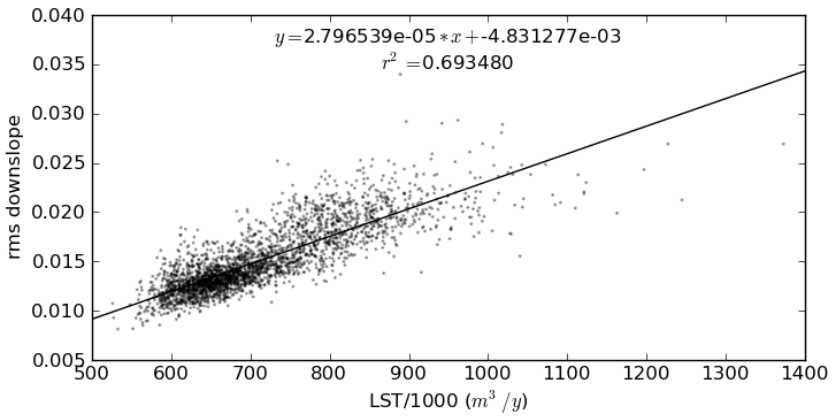

Figure 6. LST rates vs. *rms* downwards slope with linear regression

Figure 7 shows the scatter for the number of bars and the linear regression result.

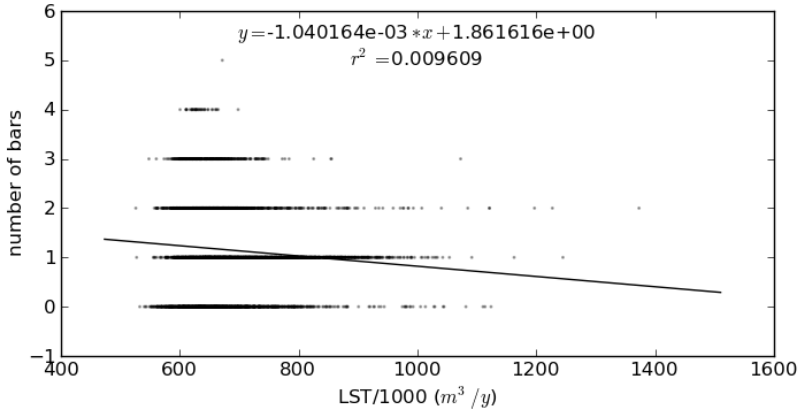

Figure 7. LST rates vs. number of bars with linear regression

Figure 8 shows the scatter for the sum of the all r_{ct} (eq.(8)) values along each profile and the linear regression.

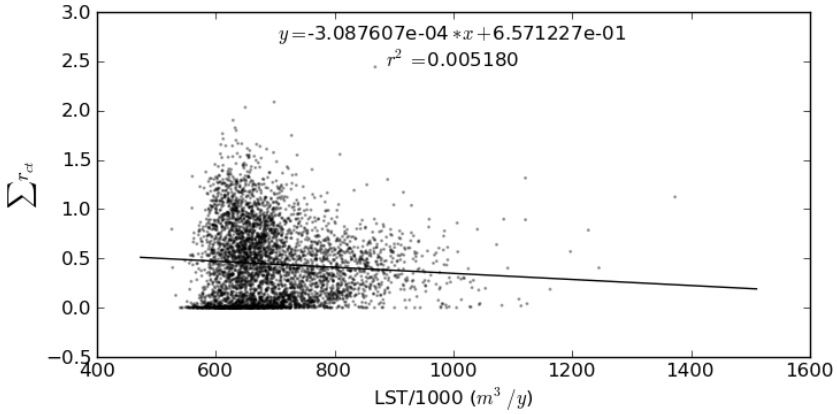

Figure 8. LST rates vs. $\sum r_{ct}$ with linear regression

In Table 4 the r^2 values obtained for all the profile features are presented.

Table 4. r^2 values for all the profile features

Profile feature	r^2
average slope	0.46
rms slope	0.60
average downwards slope	0.58
rms downwards slope	0.69
Number of bars	0.08
$\sum r_{ct}$	0.06

The calculated LST rates show significant variability with the profiles used, considering that all profiles come from the same region. In this stretch of coast the average slope values are between 0.005 and 0.02. The best correlation was found for the *root mean square* downward slope, with r^2*=0.69*. The second best was the *root mean square* slope. The other parameters related to bed slope show lower r^2 values. The *root mean square* measures seam to be better indicators for wave breaking type.

The number of bars and the other bar related parameter show no correlation with the LST rates. Nevertheless, in Figure 7 it can be seen that high transport rates only occur for 0, 1 and 2 bars. For a number of bars higher than 2, LST rates are generally low. The fact that high numbers of bars usually happen with smaller slopes may explain this result.

7. Conclusions

We tested LST rates calculated with the UNIBEST-LT model for correlations with profile related parameters.

The LST rates obtained with UNIBEST-LT vary significantly with the profile used. The percentile 95 rates were about 50% higher than the percentile 5. This is an indication that the model responds to differences in profile and that it accounts for the influence of wave breaking type in LST rates. Still, the wave climate may also exert some influence and favour LST in some profiles. Further simulations with different years of wave measurements would help us to be more certain that these differences are not an effect of the wave climate used.

The *root mean square* downward slope showed the best correlation with the calculated LST rates and all

parameters directly related with slope showed some correlation. The parameters related to the presence of bars resulted in very small r^2 values. The number of bars was found to give an indication of the potential to have higher LST rates (considering the same wave conditions): the highest rates were obtained only for profiles with 2 or less bars.

Aknowledgements

Marcel Stive, Rosh Ranasinghe and Jaap van Thiel de Vries are partly supported by the ERC-Advanced Grant 291206 – NEMO. Rosh Ranasinghe is also partly supported by "Deltares Strategic Research Programme on Coastal Developments (Bouwen aan de Kust; project number 1205871). João Mil-Homens' PhD is funded by Fundação para a Ciência e a Tecnologia.

References

Battjes, J.A., 1974. Surf Similarity. *Proceedings of the 14th International Conference on Coastal Engineering*, 1, pp.466–480.

Bayram, A., Larson, M. & Hanson, Hans, 2007. A new formula for the total longshore sediment transport rate. *Coastal Engineering*, 54(9), pp.700–710.

Bodge, K., 1986. *Short term impoundment of longshore sediment transport*,

CERC, 1984. *Shore Protection Manual*, Vicksburg: Coastal Engineering Research Center, USACE.

Deigaard, R., Fredsoe, J. & Hedegaard, I., 1986. Mathematical-model for littoral drift. *Journal of Waterway Port Coastal and Ocean Engineering -ASCE*, 112(3), pp.351–369.

Hanson, H., 1989. GENESIS - a generalized shoreline change numerical model. *Journal of Coastal Research*, 5(1), pp.1–27.

Hinton, C. & Nicholls, R., 1998. Spatial and temporal behaviour of depth of closure along the Holland coast. *Coastal Engineering Proceedings*, pp.2913–2925.

Kamphuis, J.W., 1991. Alongshore sediment transport rate. *Journal of Waterway, Port, Coastal, and Ocean …*, 117(6), p.624.

Kamphuis, J.W. et al., 1986. Calculation of littoral sand transport rate. *Coastal Engineering*, 10(1), pp.1–21.

Kamphuis, J.W. & Readshaw, J.S., 1978. A model study of alongshore sediment transport rates. *Coastal Engineering Proceedings*, pp.1656–1674.

Longuet-Higgins, M.S., 1970. Longshore Currents Generated by Obliquely Incident Sea Waves, 1. *Journal of Geophysical Research*, 75(33), p.PP. 6778–6789.

Melville, W.K., Veron, F. & White, C.J., 2002. The velocity field under breaking waves: coherent structures and turbulence. *Journal of Fluid Mechanics*, 454, pp.203–233.

Mil-Homens, J. et al., 2013. Re-evaluation and improvement of three commonly used bulk longshore sediment transport formulas. *Coastal Engineering*, 75, pp.29–39.

Rijn, L. van, 2007a. Unified view of sediment transport by currents and waves. I: Initiation of motion, bed roughness, and bed-load transport. *Journal of Hydraulic Engineering*, (June), pp.649–667.

Rijn, L. van, 2007b. Unified View of Sediment Transport by Currents and Waves. II: Suspended Transport. *Journal of Hydraulic Engineering*, 133(6), pp.668–689.

Rijn, L. van, 2007c. Unified view of sediment transport by currents and waves. III: Graded beds. *Journal of Hydraulic Engineering*, (July).

Smith, E.R. et al., 2009. Dependence of Total Longshore Sediment Transport Rates on Incident Wave Parameters and Breaker Type. *Journal of Coastal Research*, 25(3), pp.675–683.

Stive, M. J. F. & Battjes, J.A., 1984. A Model for Offshore Sediment Transport. In Houston.

Ting, F.C.K., 2001. Laboratory study of wave and turbulence velocities in a broad-banded irregular wave surf zone. *Coastal Engineering*, 43(3–4), pp.183–208.

Vitale, P. & MBLWHOI Library, 1981. *Movable-bed laboratory experiments comparing radiation stress and energy flux factor as predictors of longshore transport rate*, Fort Belvoir, Va.: U.S. Army, Corps of Engineers, Coastal Engineering Research Center; Springfield, Va.: National Technical Information Service, Operations Division [distributor].

WL|Delft Hydraulics, 1992. *UNIBEST, A software suite for simulation of sediment transport processes and related morphodynamics of beach profiles and coastline evolution. Model description and validation.*,